

SwRI Project No. 15-8087
December 31, 1998

Technical Report for

Particle Detectors and Data Analysis for Cusp Transient Features Campaign

Reference: Grant NAG5-5084

15-85
002.552

Prepared by:

James R. Sharber, Principal Investigator
Southwest Research Institute
6220 Culebra Road
San Antonio, TX 78238-5166

Submitted to:

Mr. William B. Johnson
Code 810.0
GSFC/Wallops Flight Facility
Wallops Island, VA 23337



SOUTHWEST RESEARCH INSTITUTE
Instrumentation and Space Research Division
6220 Culebra Road, San Antonio, Texas 78238
(210) 684-5111 • FAX (210) 647-4325

Technical Report on NASA Grant NAG5-5084: Particle Detectors and Data Analysis for Cusp Transient Features Campaign

ABSTRACT

On December 3, 1997, a rocket payload (36.152) was launched from Ny Alesund into the dark cusp at 0906:00 U (1206:00 LT) during an interval of southward B_z and positive B_y . Launch occurred during a time interval of northeastward moving auroral forms observed between 0845 and 0945 UT by ground-based meridian scanning photometers. Ground photometric measurements during the flight show that the payload passed over the poleward portion of the most intense 6300 Å emissions of the dayside cusp/cleft region. Electrons of energy up to a few hundred eV were detected immediately upon instrument turn-on at an altitude of 205 km and throughout the flight until the payload reached an altitude of ~197 km on the downleg. Electron spectra were either quasithermal with peak energies ~100 eV or showed evidence of acceleration along the magnetic field line by potentials of 100-200 V. Precipitating ions were observed throughout much of the flight. Their spectra were broadly peaked in energy with the peak energy decreasing from ~500 eV to ~250 eV as the payload flew approximately westward over the dayside precipitation region. Structure (spatial or temporal intensity variation) was observed between $T + 180$ s and $T + \sim 400$ s. At the rocket altitudes (<450 km) the ions were observed to be precipitating. During the flight, the DMSP F-13 satellite passed through the all-sky imager field-of-view just poleward of the brightest dayside emissions enabling the identification of plasma sheet and boundary layer regions along the orbit. We thus conclude that particle fluxes detected by the rocket flight were either cusp plasma or boundary layer/mantle plasma just poleward of the dayside cusp/cleft. Further investigation of the particle characteristics and their relationship to ionospheric convection patterns is continuing.

BACKGROUND

Grant NAS5-5084 was awarded to support the participation of SwRI in building the energy per unit charge particle detectors for the Cusp Transient Features Campaign and analysis of flight data from these instruments. The detectors were part of an instrumented payload (Rocket 36.152, Dr. R. Pfaff, P.I.) launched from Svalbard on December 3, 1997, into the dark cusp. The particle instruments, a Cusp Electron Detector (CED) and a Cusp Ion Detector (CID), built on this project, provided differential energy and angular measurements along the rocket trajectory throughout the flight.

ACCOMPLISHMENTS OF THIS PERIOD

During the past period (April 20, 1998 to December 31, 1998) we held a data workshop at the MCI facility in Nashua, New Hampshire and prepared for and presented papers at the Fall Meeting of the AGU. Both the workshop and preparation for the AGU meeting involved reduction and analysis of the CID and CED particle data and analysis of that data with other data from the flight, for example optical observations and the particle data from a nearby pass of the DMSP F-13 satellite. We have received a no-cost extension in order to continue our analysis in preparation for a publication of our flight results. In the following subsections we present our findings to date.

Flight of NASA Payload 36.152

Instrumentation

The Cusp Ion and Electron Detectors (CID and CED) are spherical tophat energy per unit charge analyzers designed to measure differential spectra over the energy range of 10 eV to 20 keV. Photos made during final instrument assembly (just before the trip to Svalbard) are shown in Figure 1. During instrument operation, a 32 point energy spectrum was measured every 0.231 s for electrons and every 0.462 s for ions. The sensing elements are Galileo microchannel plates (MCPs) arranged in Chevron configuration. Counts are sensed by an array of 24 anodes placed beneath the annulus-shaped MCPs, each anode segment defining a field-of-view of 15° in azimuth x 13° in elevation in the rocket frame. Each anode has its own discrete amplifier, an Amptek 111-F. Instrument characteristics of CID and CED are shown in the accompanying table.

IMF Conditions and Auroral Activity at Time of Launch

As a part of the Svalbard Cusp Campaign, the "Pfaff payload" (36.152) was launched from Ny Alesund (78.8° N. Lat., 75° IL) on a Black Brant IX rocket at 0906:00 UT on December 3 (Day 337), 1997 into the dayside cusp/cleft region. The IMF had a B_z component of ~ -2 nT and a B_y component of about 4 nT. Figure 2 shows the WIND solar wind data for a portion of December 3. The payload reached an apogee of 447 km and passed over the poleward portion of the main dayside precipitation region. Launch occurred after the observation of the midday auroral gap (green line absent) between 0750 and 0845 UT (1100-1200 MLT) within a time of northwestward moving auroral forms during 0845 and 0945 (Sandholt et al., 1998a; 1998b).

Electron Measurements

When CED high voltage was turned on (at $\sim T+110$ s), it immediately began to measure electrons of energies up to a few hundred eV. Several low-energy auroral "arcs" or arc-like structures were seen during the flight starting at about $T+122$ s. These are easily seen in the plot of Figure 3 (upper panel), which shows CED sector 4, one of the 24 CED sensors. The plot is an energy time spectrogram showing differential energy flux ($\text{erg/cm}^2 \text{ s sr eV}$) vs. time, with altitude, latitude, longitude, and flight time shown below the plot.

The enhancements are embedded in a less-structured background of electrons having energies up to a few hundred eV (typically 400 eV). These electrons were detected until approximately $T + 585$ s at which time the payload altitude was ~ 200 km. The altitude suggests that the payload passed below the loss height for the few-hundred eV electrons being measured. Thus this may not represent a spatial boundary.

Electron spectra are shown in Figure 4. The spectra of Figure 4a were measured at 0910:(19-21) UT, within the enhancement region seen between 0909:30 and 0910:40 UT on the spectrogram. They suggest acceleration by a field-aligned potential difference of 150-200 V. They may be compared with those measured at 0911:(15-16) UT, measured in a region of unaccelerated electrons (Figure 4b).

CID/CED* CHARACTERISTICS

ANALYZER TYPE: Tophat Energy per Unit Charge Analyzer (one for electrons, one for ions)

TOPHAT ANGLE = 17°

DEFLECTION PLATES: $R_1 = 31.25 \text{ mm}$
 $R_2 = 33.75 \text{ mm}$
 $R_3 = 36.25 \text{ mm}$

ENERGY RANGE: $10 \text{ eV} < E < 20 \text{ keV}$

ENERGY RESOLUTION: $\Delta E/E = 24\%$

DEFLECTION SENSITIVITY: $k = 6.2$

FOV: $13^\circ \times 360^\circ$ (24 angular sectors, each 15° , equally spaced)

GEOMETRIC FACTOR:

Electrons: $1.53 \times 10^{-3} \text{ cm}^2 \text{ sr}$ (per 15° sector)
Ions: $5.05 \times 10^{-3} \text{ cm}^2 \text{ sr}$ (per 15° sector)

PARTICLE SENSOR: Microchannel Plates (Chevron configuration)

NUMBER OF ANODES: 24

ENERGY STEPS: 32 (equally spaced in log of energy)

TIME RESOLUTION:

Electrons: 230.4 ms per energy scan, 7.2 ms per energy step
Ions: 460.8 ms per energy scan, 14.4 ms per energy step

DATA RATE: (after log compression from 16 to 10 bit words in DPU)

CED: 32 kbit/s
CID: 16 kbit/s

MASS: 2.5 kg each (includes deflection system, processing electronics, power supplies, and electronic box)

*CID = Cusp Ion Detector

CED = Cusp Electron Detector

Ion Measurements

The lower panel of Figure 3 shows ions measured by CID sector 4. The ion data have been processed to remove environmental noise. Precipitating ions are observed between $T + \sim 160$ s and $T + \sim 480$ s. The ion spectra were broadly peaked in energy with the peak energy decreasing from ~ 500 eV to ~ 250 eV as the payload flew approximately westward. Structure (intensity variation) is observed between $T + 180$ s and $T + \sim 400$ s. The noise starting at about $T + 400$ s results from the ACS firing.

A portion of the ion data from CID sector 4 measured between 0910:00 UT and 0911:42 UT ($T + 240$ s to $T + 342$ s) is shown in Figure 5. The top panel is an energy-time spectrogram showing the ion measurements for this time interval. The scale to the right indicates the magnitudes. In general the precipitating ions are most intense in the energy range of several hundred eV, peaking at 300-400 eV near the beginning of this interval and around 200 eV near the end. Also seen in this panel are low-energy (3-10 eV) ions moving upward along the magnetic field lines. (Pitch angles are shown in the second panel.)

The lower panel shows two parameters: (1) integrated energy flux, in units of $\text{erg/cm}^2 \text{ s sr}$ and (2) pitch angle (zero degrees = downcoming). Comparing the two curves shows clearly that the ions between 20 eV and 4 keV are precipitating. The times shown below the lower panel are UT in the top row and flight time in the second row.

The angular distribution of the ions is consistent with the low altitude of the measurement (< 450 km). The angular distributions seen at much higher altitudes on Dynamics Explorer 1 (Burch et al., 1982) are not observed due to losses resulting from atmospheric interactions below the rocket.

Comparison with Optical Measurements

During the flight, measurements were made by the Air Force ground-based all-sky imaging photometer measuring 6300 Å and 5577 Å emissions. The 6300 Å image made at 0909:34 UT is shown in Figure 6. An emission height of 230 km (based on the electron spectra) was assumed in processing the image. Also shown in the figure are the rocket and DMSP F-13 trajectories mapped down the local magnetic field lines to 230 km. The locations of the payload and DMSP are indicated by small circles on each trajectory. It is clear that the rocket trajectory passed over a portion of the 6300 Å illumination at least during the first few minutes after CED turn-on at 0907:50 ($T = 110$ s).

A spectrogram of electrons and ions measured by the DMSP F-13 is shown in Figure 7. The satellite passed through the evening/afternoon sector auroral regions (~ 16 MLT), crossed the dayside noon sector just poleward of the brightest dayside emissions, then passed through the auroral morning sector at about 09 MLT. Fluxes measured by F-13 and aboard the rocket were similar, except that on DMSP they were generally lower in intensity and energy. This is consistent with the poleward displacement of the spacecraft orbit with respect to the dayside emissions in the field of view of the photometer.

The electron and ion populations measured by DMSP F-13 show both species along the entire path of the satellite. The presence of the ions indicates that the observed fluxes are not polar cap fluxes. Rather they must be associated with the boundary layers adjacent to the cusp/cleft region. On Figure 6 we have indicated the regions immediately poleward of the plasma sheet populations (PS) as boundary layer (BL). These are regions characterized by relatively high intensities but energies less than those of the plasma sheet. These boundary layers are labeled on Figure 6 as extending between 0906:30 and 0908:00 UT and between 0911:15 and 0912:00 UT. They are the transition regions between the plasma sheet and the highest latitude populations.

Cusp and Related Precipitation

This pass of DMSP F-13 shows some similarities to that reported by Farrugia et al. (1998) in which F-13 passed over Ny Alesund. Comparisons of the DMSP particle and ground-based scanning photometer measurements, the authors associated a staircase signature in the ion precipitation structure with a series of reconnection bursts at the low-latitude dayside magnetopause. During that observation B_y was positive and the dominant IMF component (as is the case during flight 152.36), with B_z small and negative, approaching zero. Solar wind pressure and speed were very stable, somewhat more stable than during this Svalbard flight.

The boundary region encountered as F-13 passes outside the all-sky imager field of view (lower left in Figure 6, right in Figure 7) shows some signatures of the cusp, defined here in the sense of Stasiewicz (1991) as a restricted region ($\frac{1}{2}^\circ$ to 1° in extent) the surface onto which all magnetopause field lines map. In the vicinity of such a structure particle signatures show a narrow "V-shaped" signature in the ion spectrogram and evidence of upward field aligned currents in the low-energy electrons. These signatures are suggested in the F-13 spectrogram near 0912 UT (10:15 MLT). Support based on other data, such as electric and magnetic field signatures will be required to test these interpretations.

Flight Summary

- On December 3, 1997, a rocket payload (36.152) was launched from Ny Alesund into the dark cusp at 0906:00 UT (1206:00 LT) during an interval of southward B_z and positive B_y .
- Launch occurred during a time interval of northwestward moving auroral forms observed between 0845 and 0945 UT by ground-based meridian scanning photometers.
- Ground photometric measurements during the flight show that the payload passed over the poleward portion of the most intense 6300 Å emissions of the dayside cusp/cleft region.
- Electrons of energy up to a few hundred eV were detected immediately upon instrument turn-on at an altitude of 205 km and throughout the flight until the payload reached an altitude of ~197 km on the downleg. Electron spectra were either quasithermal with peak energies ~100 eV or showed evidence of acceleration along the magnetic field line by potentials of 100-200 V.

- Precipitating ions were observed throughout much of the flight. Their spectra were broadly peaked in energy with the peak energy decreasing from ~500 eV to ~250 eV as the payload flew approximately westward over the dayside precipitation region. Structure (spatial or temporal intensity variation) was observed between T + 180 s and T + ~400 s. At the rocket altitudes (<450 km) the ions were observed to be precipitating.
- During the flight, the DMSP F-13 satellite passed through the all-sky imager field of view just poleward of the brightest dayside emissions enabling the identification of plasma sheet and boundary layer regions along the orbit.
- We thus conclude that particle fluxes detected by the rocket flight were either cusp plasma or boundary layer/mantle plasma observed just poleward of the dayside cusp/cleft.
- Further investigation of the particle characteristics and their relationship to ionospheric convection patterns is continuing.

PRESENTED PAPERS

The grant has supported work on the following presented papers. Item 4 below is appended to this report.

1. Bounds, Scott R., R. F. Pfaff, Jr., K. Masiede, N. C. Maynard, J. Sharber, M. Coplan, J. Clemmons, D. Hardy, H. Freudenreich, J. Moen, A. Egeland, P. E. Sandholt, J. Moore, W. Burke, P. Ning, E. Weber, M. Lockwood, A. B. Van Eiken, M. Lester, and S. Milan, Thermal ionization observed by instruments on two sounding rockets launched in the dark dayside cusp, presented at the Fall AGU Meeting, abstract *EOS Trans. Supplement*, **79**, F777, 1998.
2. Coplan, M. A., J. H. Moore, N. Zukerman, J. H. Clemmons, J. R. Sharber, R. H. Pfaff, Ion fluxes in the region of the polar cusp, presented at the Fall AGU Meeting, abstract *EOS Trans. Supplement*, **79**, F777, 1998.
3. Pfaff, R., Jr., *et al.*, DC and wave electric fields and other plasma parameters observed on two sounding rockets in the dark cusp during IMF B_z north and south conditions, presented at the Fall AGU Meeting, abstract *EOS Trans. Supplement*, **79**, F777, 1998.
4. Pope, S. E., J. R. Sharber, R. A. Frahm, M. Grande, A. Preece, M. A. Coplan, J. H. Clemmons, R. E. Sandholt, P. Ning, E. J. Weber, and R. H. Pfaff, Jr., Rocket measurements of electron and positive ions during the Svalbard cusp campaign, presented at the Fall AGU Meeting, abstract *EOS Trans. Supplement*, **79**, F780, 1998.

WORK REMAINING

During the next six months we will continue to analyze the particle data in order to be able to use the particle spectra as inputs to ionization production rate codes. A secondary goal is to determine the intensities and energies of the ions at the top of the atmosphere. The first of these tasks is essential for determining emission heights which are required for mapping auroral features from the all-sky camera images into geographic or geomagnetic coordinates. They are modeling tasks that may require additional funding for completion.

Noise removal from the CID (ion) data will continue. It now appears that, as a result of the noise, only about half of the CID sensors are usable. However, the unexpected coning of the payload allows very good angular scans from several of these sensors. We plan to modify existing analysis programs in order to produce angular distribution plots of the ion data.

REFERENCES

Burch, J. L., P. H. Reiff, R. A. Heelis, J. D. Winningham, W. B. Hanson, C. Gurgiolo, J. D. Menietti, R. A. Hoffman, and J. N. Barfield, Plasma Injection and transport in the mid-altitude polar cusp, *Geophys. Res. Lett.*, **9**, 921-924, 1982.

Farrugia, Charles J., Per Even Sandholt, William F. Denig, and Roy B. Torbert, Observation of a correspondence between poleward moving auroral forms and stepped cusp ion precipitation, *J. Geophys. Res.*, **103**, 9309-9315, 1998.

Newell, Patrick T., William J. Burke, Ching-I. Meng, Ennio R. Sanchez, and Marian E. Greenspan, Identification and observations of the plasma mantle at low altitude, *J. Geophys. Res.*, **96**, 35-45, 1991.

Pope, S. E., J. R. Sharber, R. A. Frahm, M. Grande, A. Preece, M. A. Coplan, J. H. Clemmons, R. E. Sandholt, P. Ning, E. J. Weber, and R. H. Pfaff, Jr., Rocket measurements of electron and positive ions during the Svalbard cusp campaign, presented at the Fall AGU Meeting, abstract *EOS Trans. Supplement*, **79**, F780, 1998.

Sandholt, Per Even, Charles J. Farrugia, Joran Moen, Oystein Norberg, Bjorn Lybekk, Torleif Sten and Truls Hansen, A classification of dayside auroral forms and activities as a function of interplanetary magnetic field orientation, *J. Geophys. Res.*, **103**, 23325-23345, 1998a.

Sandholt, Per Even, Charles J. Farrugia, J. Moen, Stanley W. H. Cowley, and B. Lybekk, Dynamics of the aurora and associated convection currents during a cusp bifurcation event, submitted to *Geophys. Res. Lett.*, 1998b.

Stasiewicz, K., A global model of gyroviscous field line merging at the magnetopause, *J. Geophys. Res.*, **96**, 77-86, 1991.

FIGURE CAPTIONS

Figure 1. Views of CID/CED instrument.

Figure 2. Data from WIND spacecraft at L1.

Figure 3. CED and CID energy-time spectrogram showing differential energy flux ($\text{erg/cm}^2 \text{ s sr eV}$) vs. time, with altitude, latitude, longitude, and flight time shown below the plot.

Figure 4. Electron spectra measured during the flight.

Figure 5. Cusp Ion Detector (CID) spectrogram (top panel) showing measurements between 0910:00 UT and 0911:42 UT ($T + 240\text{s}$ to $T + 342\text{s}$). Energy flux and pitch angle are plotted in lower panel.

Figure 6. All-sky image of 630 nm emissions above Ny Alesund with rocket and DMSP trajectories mapped to 250 km.

Figure 7. DMSP F-13 electron and ion spectrogram.

Appendix: Fall AGU Poster (Pope *et al.*, 1998)

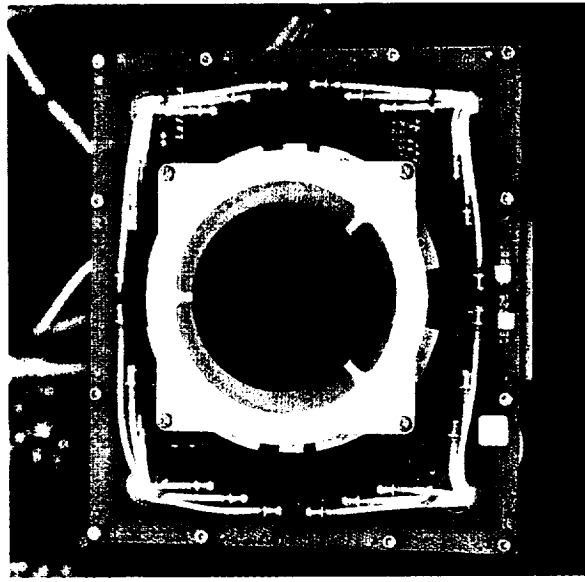
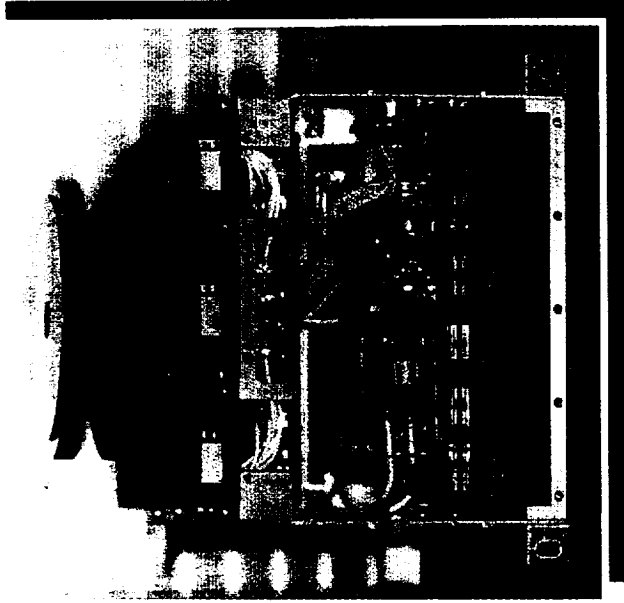
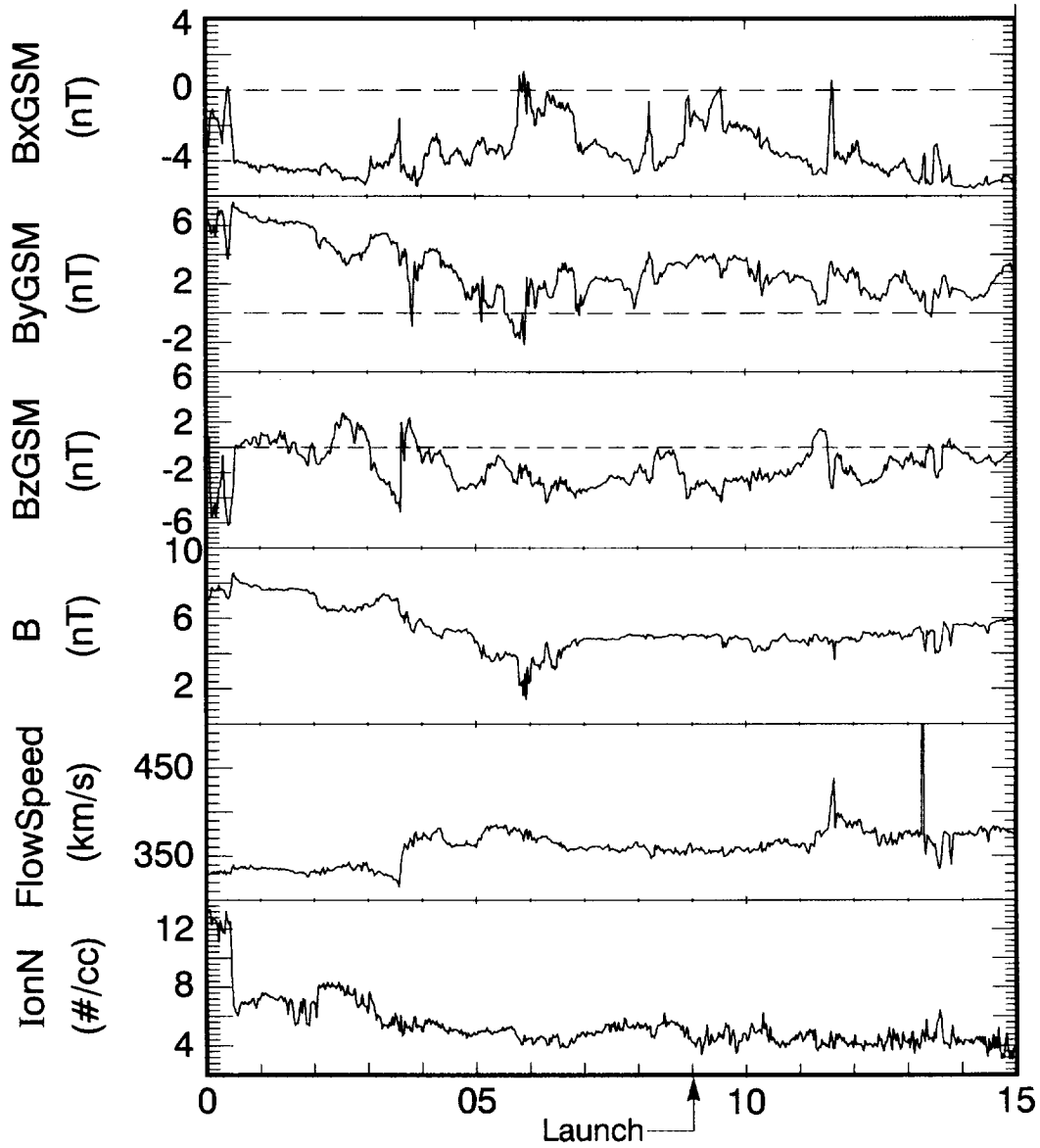


Figure 1

WIND DATA

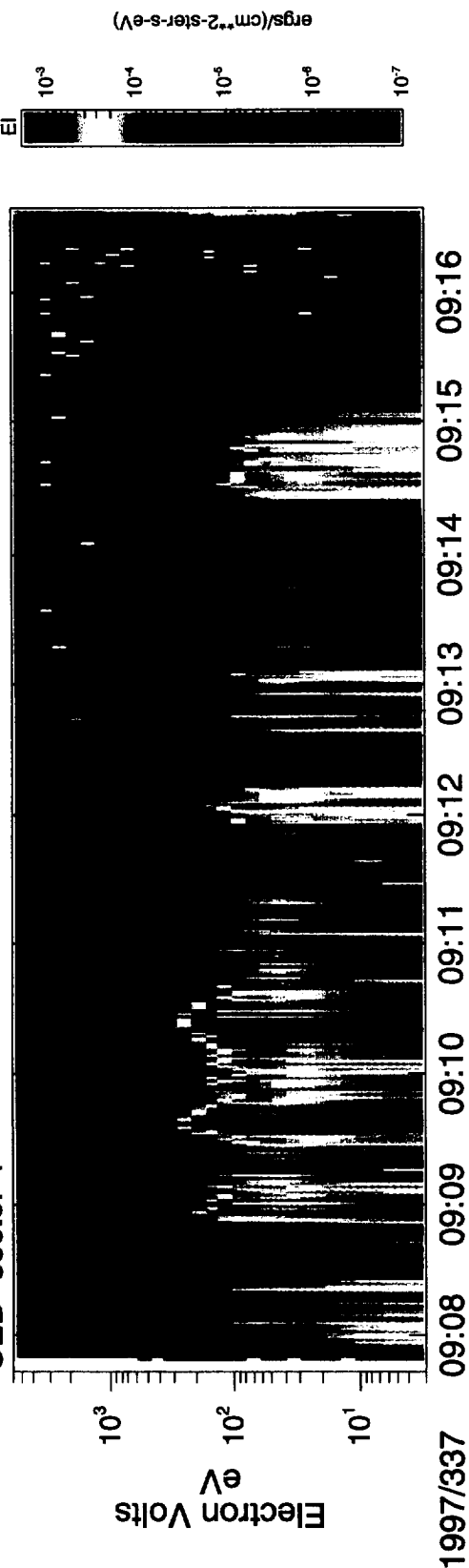


DEC 03, 1997 UT Hours

Figure 2

SVALBARD 36.152

CED -sector 4



CID sector 4

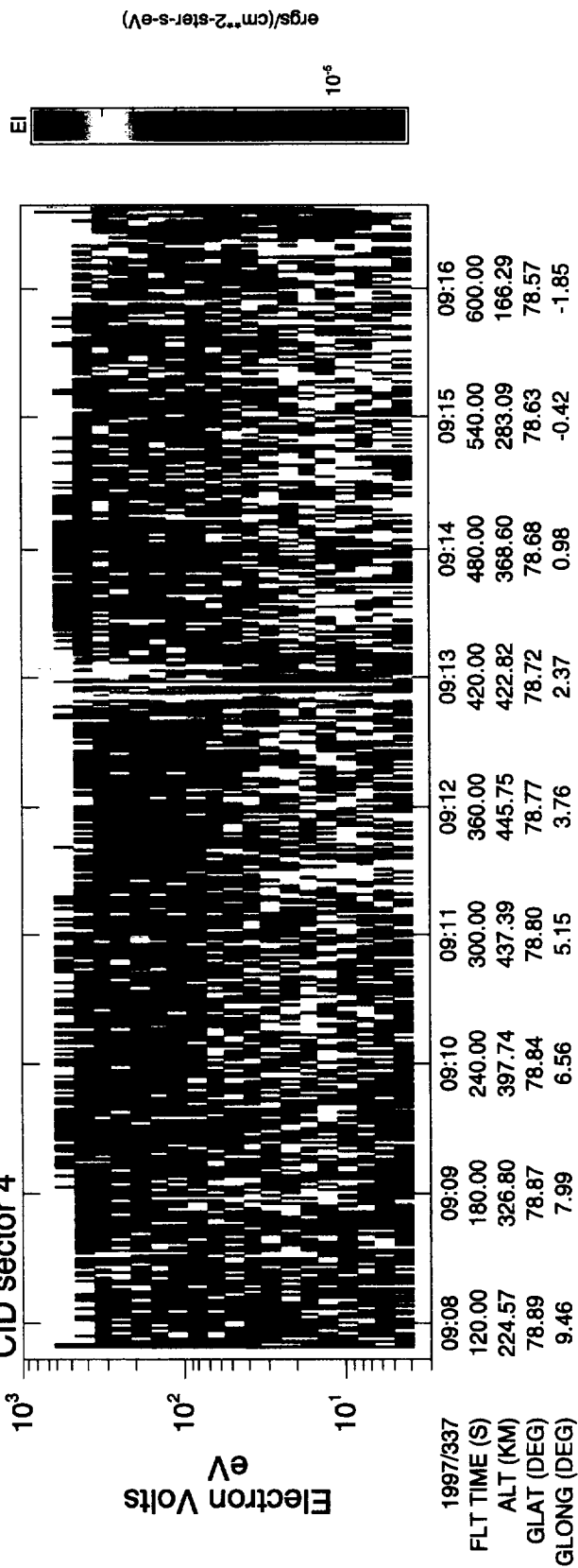
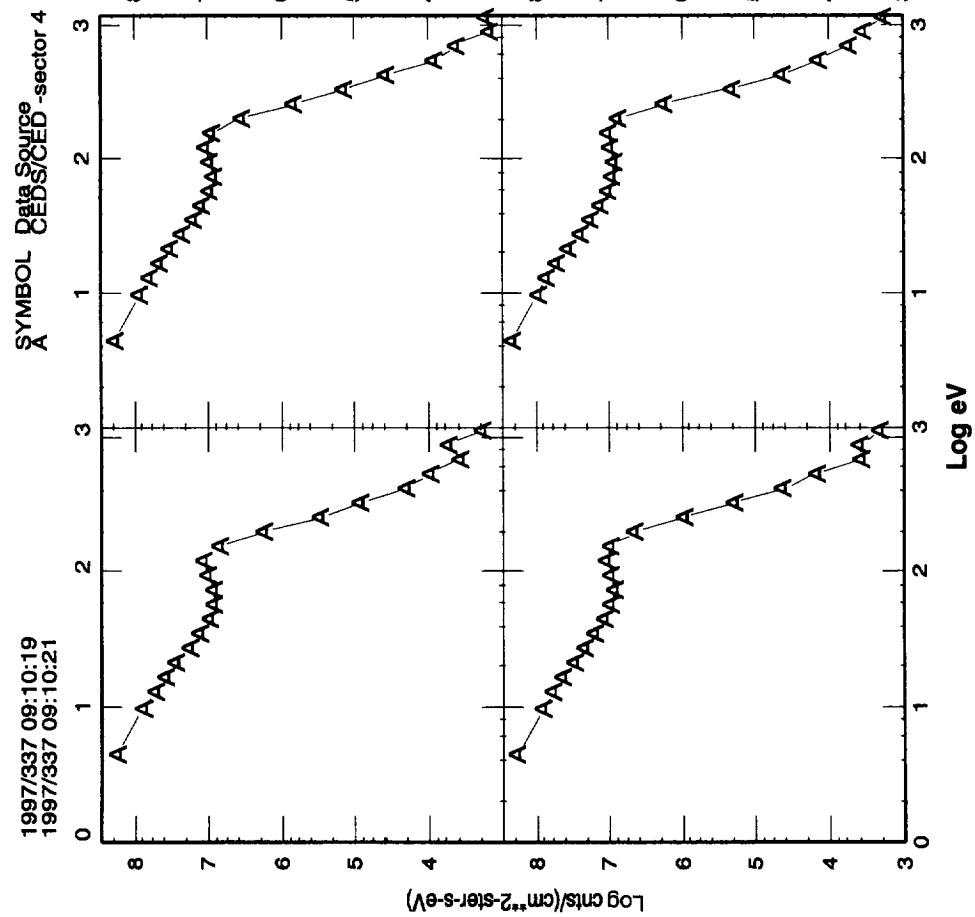
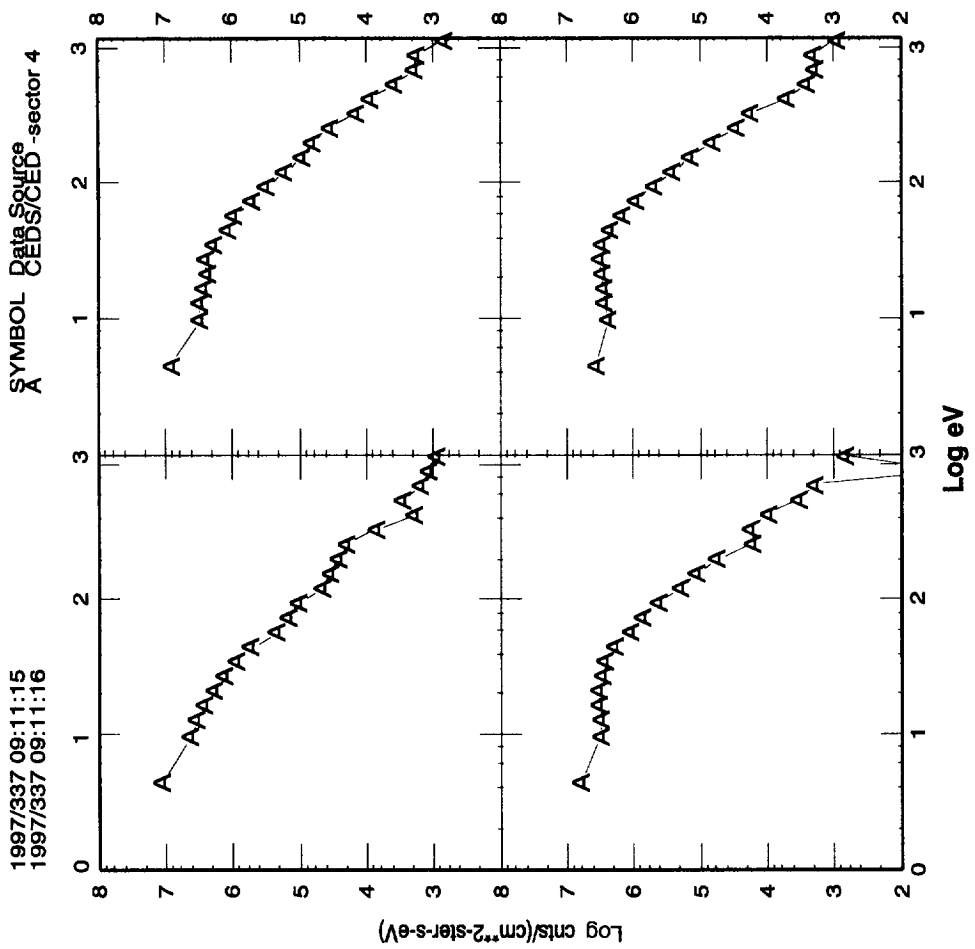


Figure 3



a

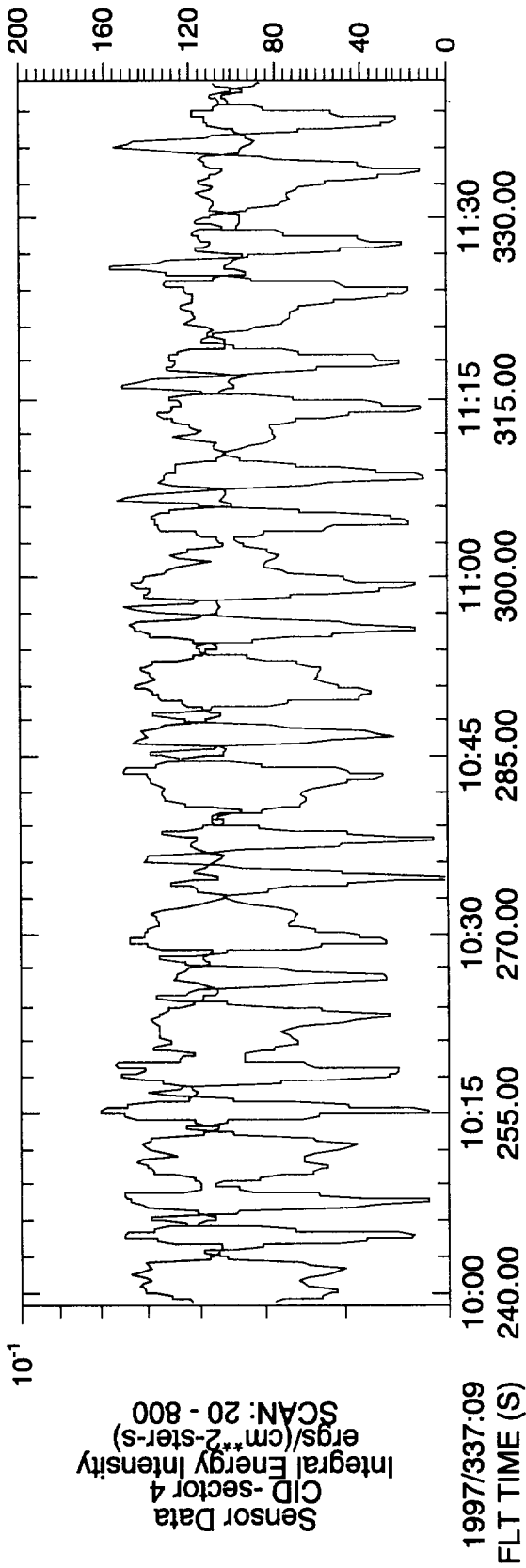
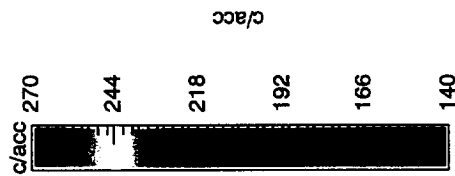
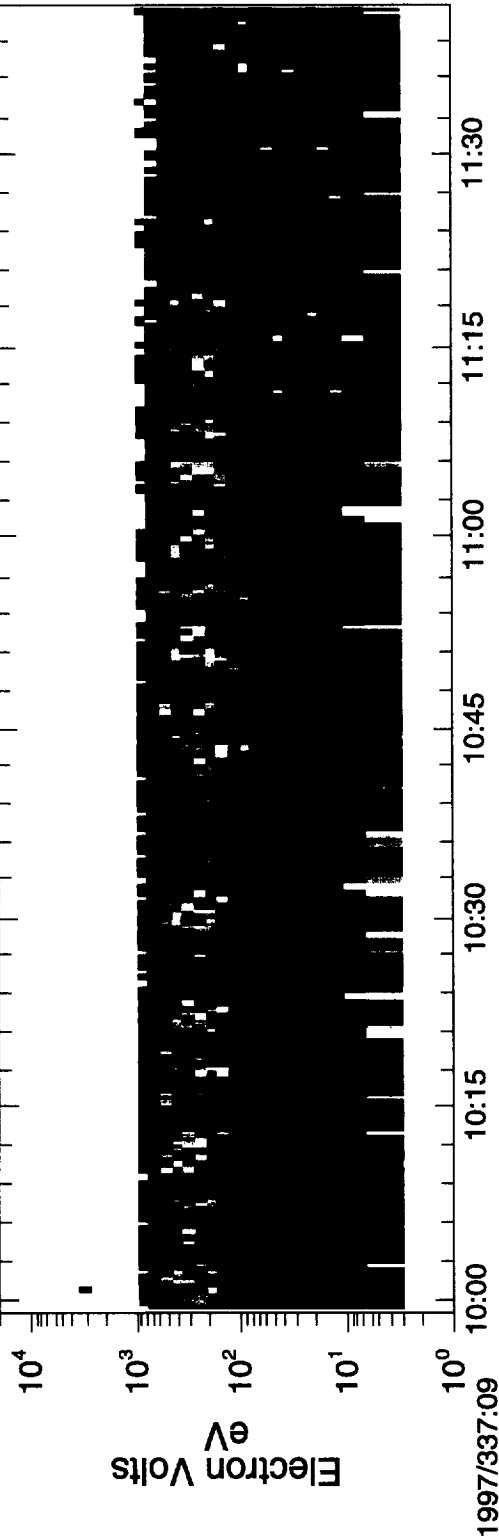


b

Figure 4

SVALBARD 36.152

CID -sector 4



Pitch Angle/020
CID -sector 4
Pitch Angle
Degrees

Figure 5

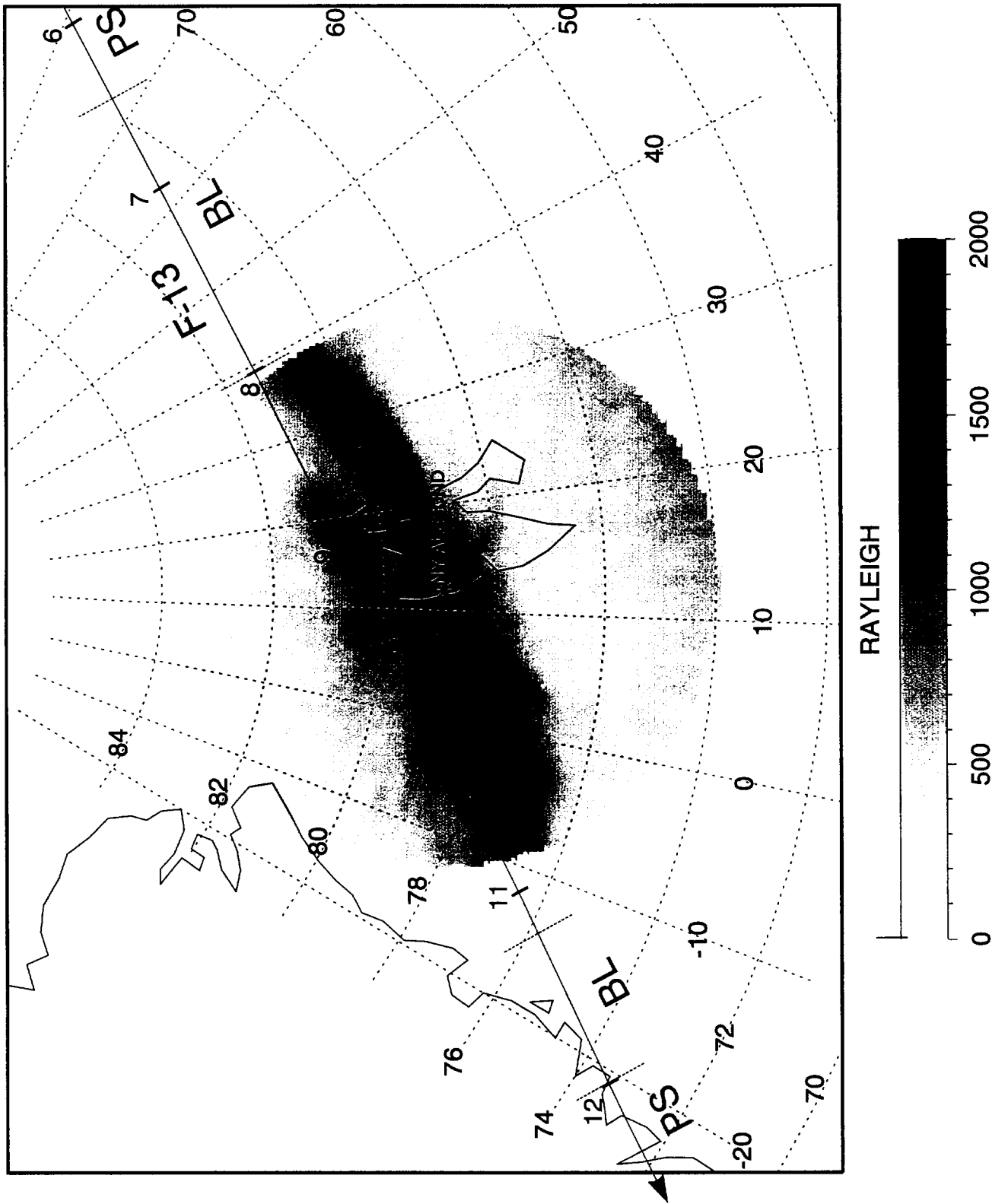
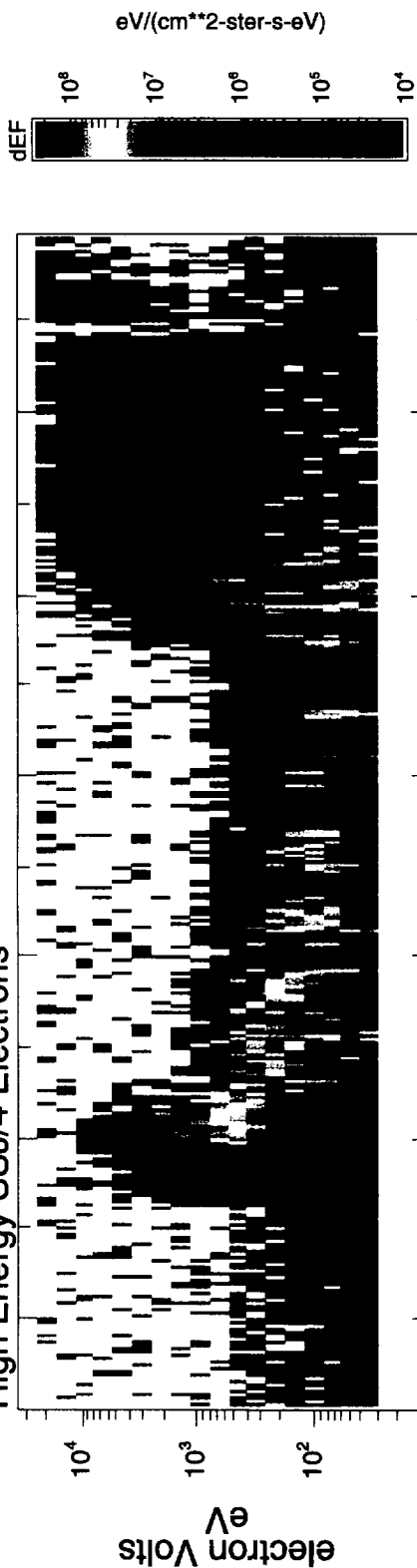


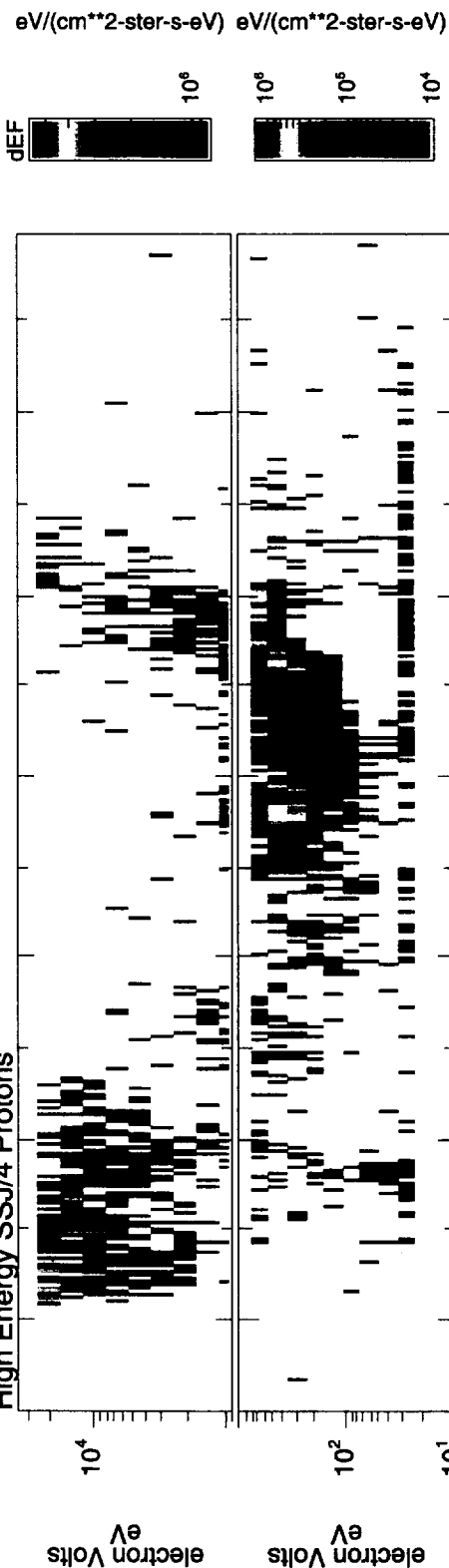
Figure 6

DMSP F-13

Low Energy SSJ/4 Electrons
High Energy SSJ/4 Electrons



High Energy SSJ/4 Protons



1997/337	09:04	09:06	09:08	09:10	09:12	09:14
ILAT	67.41	72.74	76.30	76.87	74.26	69.50
MLT	16.27	15.33	13.81	11.83	10.15	9.07
GDLAT	73.60	78.90	81.20	78.60	73.30	67.00
GDLONG	99.20	78.50	38.60	359.80	340.10	330.00
	67.70	72.70	76.60	77.70	75.20	70.50

Figure 7

